



propagation within each optical medium was modeled with an extended nonlinear Schrödinger equation that accounts for the effects of GVD, third-order dispersion, and Kerr nonlinearity with a Raman contribution, including gain for the Yb-doped fiber. All the parameters in the model were known from experiment. Gain in the Yb-doped fiber was modeled as saturating with total energy and has a parabolic frequency dependence with a bandwidth of 40 nm.

The quantitative agreement between calculated and measured laser performance with large anomalous GVD allowed us to optimize the laser efficiently. Starting from this point, numerical simulations revealed the expected trend of increasing maximum single-pulse energy with dispersion decreasing in magnitude to zero and then to increasing normal dispersion. The pulse duration and the time–bandwidth product, however, attained minima near zero dispersion. The spectrum and the temporal pulse shape diverged rapidly from a shape that resembles a Gaussian with increasing normal dispersion. The spectrum assumed a square shape, and a sinc-function temporal shape was obtained. This trend does not depend on the details of the model. Simulations provided good qualitative and quantitative agreement with all the experimental configurations that were tried. Consideration of dispersion and nonlinearity maps of the cavity, along with a saturating, finite-bandwidth gain, are sufficient for a qualitative description.

Power spectra and interferometric autocorrelations of the pulses generated from the laser with gain at the end of the fiber section are shown in Fig. 2. The three horizontal parts of the figure correspond to net GVD values of  $-0.067$ ,  $-0.038$ , and  $-0.021$  ps<sup>2</sup>. With total fiber lengths of 1.4–2.8 m, the pulse repetition rate varied from 95 to 56 MHz. Directly from the NPE port, the pulse durations were 460, 210, and 120 fs for the GVD values of Fig. 2. After dechirping, pulse durations of 300, 120, and 75 fs were measured. We could tune the center wavelength from 1020 to 1040 nm by translating an aperture in the Fourier plane between the gratings. The locations of the spectral sidebands agree well with estimates from the measured pulse duration and the calculated GVD. The sidebands diminished and the spectrum deviated from the sech shape with decreasing magnitude of GVD, as expected. A pulse energy of 0.5 nJ (before dechirping) was readily obtained with 300 mW of pump power.

With normal GVD, only *Q*-switched mode locking could be observed, even with the highest available pump power (500 mW). True mode-locked operation at normal GVD could be hindered by one of several factors: inadequate nonlinearity, an inadequate stretching ratio to support a dispersion-managed soliton with normal GVD, and a tendency toward *Q*-switched mode locking at higher repetition rates. All these effects are addressed by the addition of fiber after the gain medium, so a segment of single-mode fiber was spliced to the Yb fiber. The length of the fiber section was then 3.7 m, and the resultant repetition rate was 46 MHz.

The power spectra and autocorrelations produced by this laser with GVD close to zero are shown in

Fig. 3. The three horizontal parts of the figure correspond to net GVD values of  $-0.008$ ,  $+0.004$ , and  $+0.016$  ps<sup>2</sup>. It is clear that for these GVD values the chirp is much larger than it is with large anomalous GVD. The measured pulse durations were 280 fs, 2.8 ps, and 3.6 ps directly from the laser and 71, 52, and 143 fs (assuming Gaussian pulse shapes) after dechirping. In stable operation a pulse energy of 2.2 nJ was obtained, which is 20 times higher than that reported with earlier Yb fiber lasers. After dechirping, 100-fs, 1.8-nJ pulses can be delivered.

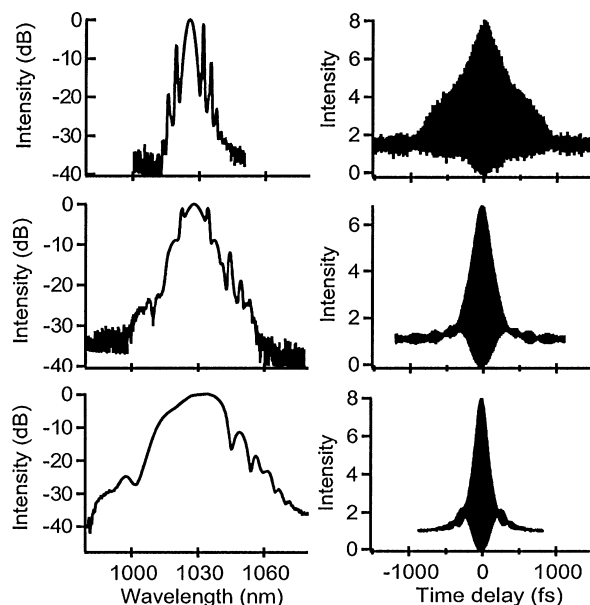


Fig. 2. Spectra (note the logarithmic scale) and interferometric autocorrelations produced by the laser with anomalous GVD. The net dispersions are  $-0.067$ ,  $-0.038$ , and  $-0.021$  ps<sup>2</sup> from top to bottom.

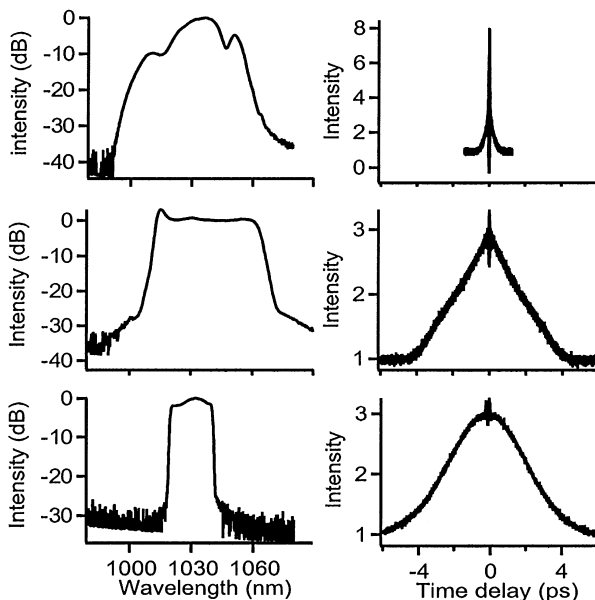


Fig. 3. Spectra and interferometric autocorrelations produced by the laser with gain in the center of the fiber section. The net dispersions are  $-0.008$ ,  $+0.004$ , and  $+0.016$  ps<sup>2</sup> from top to bottom.

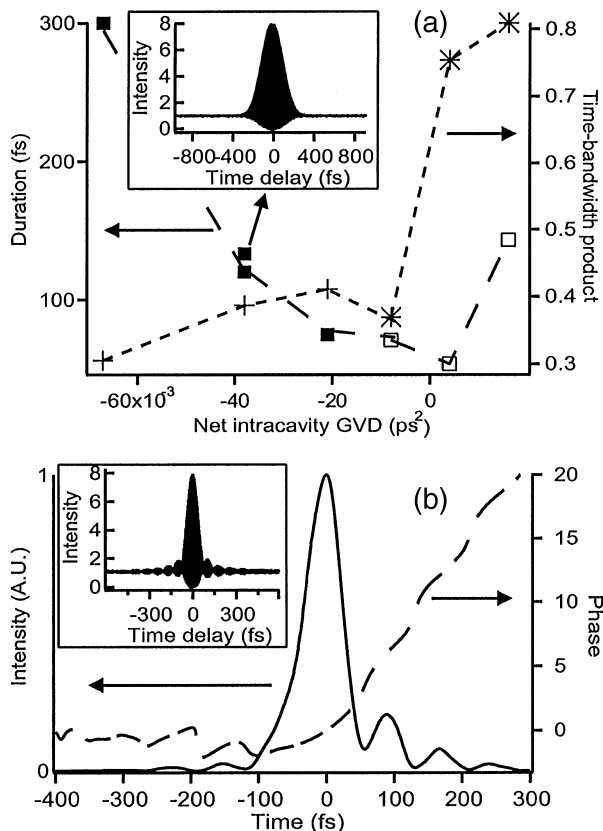


Fig. 4. Pulses after chirp compensation. (a) Pulse duration and time-bandwidth product as a function of net GVD. A Gaussian pulse shape is assumed, except for the points at  $-0.067$  and  $-0.038$  ps<sup>2</sup>, for which a sech shape was assumed. Inset, autocorrelation of a 130-fs pulse without secondary structure (see text). (b) Phase (dashed curve) and temporal intensity (solid curve) traces of the shortest pulses generated by the YB fiber laser. Inset, autocorrelation of the same pulse.

We verified single-pulse operation by monitoring (i) the pulse train with a fast detector and a sampling oscilloscope (nanosecond time scale), (ii) modulation on the spectrum ( $<10$ -ps range), and (iii) the long-range autocorrelation ( $<100$ -ps range). In addition, no continuous-wave lasing was present.

The dependence of the duration of the dechirped pulse and of the time-bandwidth product on the cavity GVD are shown in Fig. 4 along with the measurement of the shortest pulses that we have observed.

The intensities and phases of the shortest pulses were inferred by use of a pulse retrieval algorithm based on fitting the measured interferometric autocorrelation and spectrum.<sup>7</sup> The FWHM pulse duration was 52 fs. These are to our knowledge the shortest pulses produced by a Yb fiber laser. Applications such as amplification and harmonic generation would benefit from longer but cleaner pulses, which we obtained by adjusting the polarization settings [Fig. 4(a), inset].

All the laser configurations described above are self-starting. The fluctuations in pulse energy are  $\sim 0.1\%$ , and mode-locked operation is stable for weeks. The key to stable operation is the delivery of diode pump light via a wavelength-division multiplexing coupler, and the presence of the free-space section (gratings, wave plates, and polarizer) apparently does not degrade the long-term stability of the laser. Of course, a truly environmentally stable laser will require polarization-maintaining fiber or the use of Faraday rotators.

In conclusion, we have demonstrated a mode-locked Yb fiber laser and studied its performance from soliton to stretched-pulse regimes. This laser generates shorter pulses, and an order-of-magnitude higher pulse energies, than previous Yb fiber lasers. We expect that it will find numerous applications.

This study was supported by the National Institutes of Health under grant RR10075 and by Clark/MXR, Inc. The authors thank Coherent, Inc., for providing an OPSP pump laser. H. Lim's e-mail address is hl247@cornell.edu.

## References

1. M. Hofer, M. H. Ober, F. Haberl, and M. E. Fermann, *IEEE J. Quantum Electron.* **28**, 720 (1992).
2. K. Tamura, J. Jacobson, H. A. Haus, E. P. Ippen, and J. G. Fujimoto, *Opt. Lett.* **18**, 1080 (1993).
3. V. Cautaerts, D. J. Richardson, R. Paschotta, and D. C. Hanna, *Opt. Lett.* **22**, 316 (1997).
4. L. Lefort, J. H. V. Price, D. J. Richardson, G. J. Spuhler, R. Paschotta, U. Keller, A. R. Fry, and J. Weston, *Opt. Lett.* **27**, 291 (2002).
5. K. Tamura, J. Jacobson, E. P. Ippen, H. A. Haus, and J. G. Fujimoto, *Opt. Lett.* **18**, 220 (1993).
6. K. Tamura, C. R. Doerr, L. E. Nelson, H. A. Haus, and E. P. Ippen, *Opt. Lett.* **19**, 46 (1994).
7. J. W. Nicholson, J. Jasapara, W. Rudolph, F. G. Omenetto, and A. J. Taylor, *Opt. Lett.* **24**, 1774 (1999).